

Observing Oxidating Kinetics on an Aluminium Alloy Surface with Fluorescence Mapping

Metal oxides, in contrast to most metals, are well known to be easily distinguished by their characteristic Raman spectra; their presence can be detected on a scale of micrometers with a Raman microprobe. Often, the various oxides of a particular metallic ion have significantly different Raman spectra, with even the degree of hydration of the ligated cation generating a tell-tale vibrational fingerprint. Thus, the diverse oxide forms of a variety of metals, including, for example, iron, nickel, lead, titanium, zirconium, molybdenum, copper, and vanadium, can be distinguished by a fast and non-destructive spectroscopic measurement. In practice, this allows the scientist or engineer to delineate the kinetics of oxidation of any of these species, observing where and when successive species are formed during the oxidation of a raw metal. For example, steel rust exhibits layers of several oxides of iron, including hematite, lepidocrocite, goethite, and magnetite, with the layer thicknesses and ordering dependent upon the composition of the steel, the conditions of the environment, and the duration of exposure.

Aluminium metal has a wide range of technical uses, both as a pure metal and as a component in various light-weight alloys. Although it is resistant to gross oxidation (following formation of a thin protective layer of oxide) under normal ambient conditions, it can be oxidized and eroded by exposure to the higher temperatures common to furnaces and turbine engines in which various aluminium-containing alloys are used. An understanding of the kinetics of oxidation might allow passivation of the oxidation process or reasonable estimation of mean failure times for aluminium containing components.

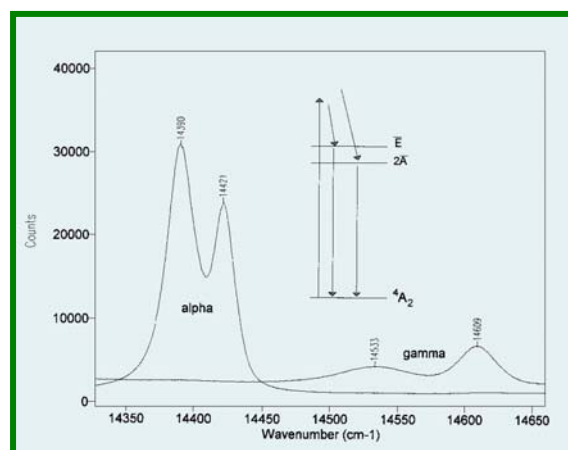


Figure 1: Comparison of fluorescence spectra of alpha and gamma phases of alumina.

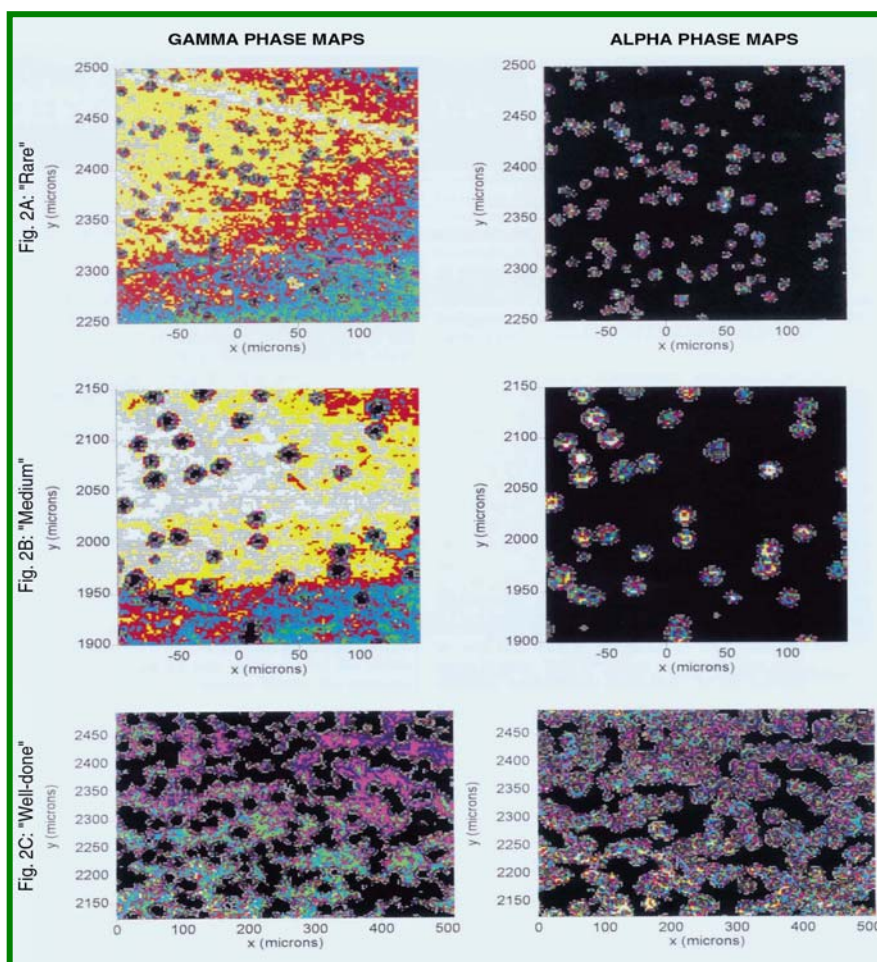
There are various forms of aluminum oxide, the alpha, beta, and gamma phases among them, so identification of the primary and secondary products of aluminum oxidation would be a starting point for an understanding of the oxidation process. Although these several oxide products do have distinguishing Raman spectra, they are more easily identified by the effect of their characteristic crystal structures upon the fluorescence of the oxidized form of the chromium which is consistently present as a trace impurity in aluminum metal. Fig.1 shows the chromium fluorescence spectra due to two forms of alumina, the alpha and gamma. The two bands in each spectrum, known as R1 and R2, are due to the radiative decay from the $2E$ and $2A$ excited states of the chromium cation to the $4A_2$ ground state.

Crystal field effects shift the energies of the two transitions, so that, as seen in the Figure, the respective phases provide distinct and non-overlapped spectroscopic signatures.

The spectral range of these fluorescence bands is narrow enough so that they can be simultaneously detected by a modern Raman spectrograph equipped with a multi-channel CCD detector. Thus, a Raman spectrometer can handily double as a fluorescence emission instrument, allowing one to monitor an aluminium surface for the presence of these two species.

The capacity to differentiate these two phases is most useful when combined with a microscopic imaging technique, which provides a concentration .map, a plot of intensity of the spectroscopic signature of a particular species as a function of position on the sample. Images can be obtained using three different methods: global imaging, point-by-point confocal imaging, and confocal line scan imaging. Global imaging is the simplest and fastest: it provides a map of intensity at a particular wavelength as a function of surface position. Although global imaging can be useful in certain circumstances, we will see in the example below that it can miss information obtained with the more thorough techniques. Point-by-point imaging

uses a motorized computer-controlled microscope stage in combination with a high power microscope objective to obtain an entire spectrum for each point on the surface; the diffraction limit of the microscope optics allows a spatial resolution of better than 1.0 micrometer. Confocal line scan imaging is a patented technique for collecting the same information as obtained by point-by-point imaging, but in significantly less time: the laser is scanned along lines on the sample surface; the light collected from each point on the line is imaged to a distinct position on the entrance slit of the spectrograph, and hence to a distinct slice of a two-dimensional CCD array detector. Reading the CCD once provides simultaneously the spectra emitted by all points on the scanned line; the sample can then be translated perpendicular to the laser scan direction to provide a two dimensional map of the surface. The example which follows presents data collected by point-by-point imaging. The same data could have been obtained, somewhat more quickly, with the line-scan technique, whereas the global imaging approach was found to be less informative.



Three single crystals of a NiAl superalloy were heated to 1100°C for 15 minutes (“rare”), 30 minutes (“medium”), and 60 minutes (“well-done”), respectively. Fig 2A shows intensity maps of the alpha and gamma phases for a “rare” sample; each successive colour corresponds to a constant maximum intensity in the spectral range characteristic of a particular phase of the oxide. The two plots are obviously complementary; the alpha phase shows maximum intensity (brightest colour) in isolated regions which correspond to minima (darkest colour) in the amps of gamma intensity. Apparently, the alpha alumina is contained in islands in a sea of the gamma polymorph. Fig. 2B shows the same comparison for a “medium” sample. While there are fewer islands here, they are somewhat larger. Finally, Fig.2C, maps of a “well-done” sample, show that the alpha nucleation sites have grown with longer exposure, to the point where they intersect with each other and approach total coverage of the mapped region. The obvious conclusion is that the gamma phase is the primary oxidation product on this surface, and the alpha phase grows following nucleation within the gamma phase.

Three dimensional views of these maps provide further information which is not immediately obvious in the above maps. Figure 3 shows 3D views of the alpha phase intensity maps shown on the right side of figure 2. Figure 3A shows that the islands in the “rare” sample are inverted cones with maxima in the centers of the islands, as one might expect. However, the islands in the “medium” sample, seen in figure 3B, are more akin to

volcanoes, with the maximum intensities between the center and the edge of the island, and a crater in the middle. Finally, figure 3C shows the same view of the “well-done” surface; the merging islands maintain their volcanic interiors. The structural nature of the craters on the interior of these volcanic islands has not yet been characterised.

Although all of these results could, in principal, have been obtained by the global imaging technique, this would require further image processing to eliminate baseline effects. However, there is information intrinsic to these data which is not obtained with global imaging. Because we have collected a full spectrum at each position in the sample, it is possible to use all the usual arsenal of spectroscopic data analysis on the data set; this includes intensity ratios, curvefitting, and multivariate analytical techniques. Other ISA technical notes have discussed the value of chemometric analysis in extracting data from complex data sets. For present purposes, the methodology of choice is curve-fitting. This is because the R1 and R2 energies are sensitive to changes in the local strain of the lattice; in fact, it is precisely this dependence that allows the fluorescence from ruby crystals to provide a pressure calibration of high-pressure cells. Here, because of the micrometer scale resolution of the probe, we are able to map changes in the strain of these islands as they grow in size. This provides a non-contact probe of the dynamic mechanical properties of the sample. These results will be demonstrated in a future technical note, which will discuss the importance of stress mapping to the characterisation of engineered materials.



Figure 3A

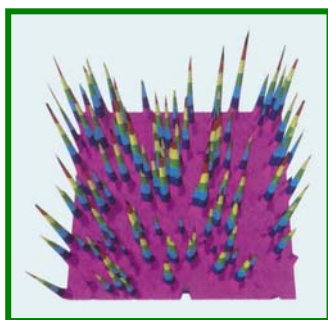


Figure 3B

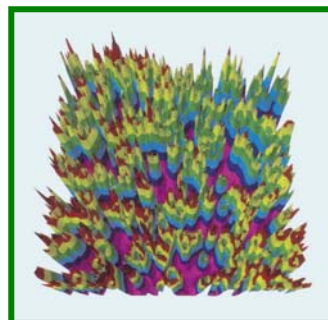


Figure 3C

Figure 3: Three dimensional views of alpha intensity maps.

HORIBAJOBIN YVON

France : HORIBA Jobin Yvon S.A.S., 231 rue de Lille, 59650 Villeneuve d'Ascq. Tel : +33 (0)3 20 59 18 00, Fax : +33 (0)3 20 59 18 08. Email : raman@jobinyvon.fr www.jobinyvon.fr
USA : HORIBA Jobin Yvon Inc., 3880 Park Avenue, Edison, NJ 08820-3012. Tel : +1-732-494-8660, Fax : +1-732-549-2571. Email : raman@jobinyvon.com www.jobinyvon.com
Japan : HORIBA Ltd., JY Optical Sales Dept., 1-7-8 Higashi-kanda, Chiyoda-ku, Tokyo 101-0031. Tel: +81 (0)3 3861 8231, Fax: +81 (0)3 3861 8259. Email: raman@horiba.com
Germany: +49 (0) 6251 84 75-0 **Italy:** +39 02 57603050 **UK:** +44 (0)20 8204 8142
China: +86 (0) 10 6849 2216